



# Nanocrystalline hydrogen storage alloys for rechargeable batteries

H. Kronberger

*Institut für Technische Elektrochemie, Getreidemarkt 9, A-1060 Wien, Austria*

## Abstract

AB<sub>5</sub>-type intermetallic compounds were prepared by the melt spinning method. Structure analysis was carried out by X-ray diffractometry, SEM and high resolution electron microscopy. The hydrogen storage capacity was determined by isothermic mass controlled absorption of hydrogen and by electrochemical charge/discharge cycles. A variation of the preparation parameters showed that a nanocrystalline structure was achieved at high cooling rates. Nanocrystalline AB<sub>5</sub>-compounds show improved electrochemical properties.

*Keywords:* Nanocrystalline; Hydride; Electrodes; Batteries; Cells

## 1. Introduction

The enhancement of grain boundary diffusion of hydrogen in polycrystalline AB<sub>5</sub>-compounds by the formation of additional phases was found to accelerate the limiting transport processes [1]. From this point of view the properties of materials in an amorphous or nanocrystalline state also are of special interest. Although thin layers of amorphous LaNi<sub>5</sub> prepared by r.f. sputtering were investigated by some authors, we were looking for a suitable method for the production of substantial amounts of amorphous or nanocrystalline material from AB<sub>5</sub>-compounds for the preparation of electrodes. Several papers have been published concerning the electrochemical behaviour of microcrystalline AB<sub>5</sub>-compounds produced by rapid solidification [2] in a melt spinning device, but apparently the cooling rates that are usually achieved with this method are too low to produce amorphous materials. Moreover, the influence of preparation parameters on the properties of these electrode materials, in particular concerning kinetic aspects, still remain unclear.

## 2. Experimental

### 2.1. Preparation and rapid solidification

Electrode materials were prepared from RENi<sub>3.5</sub>Co<sub>0.8</sub>Mn<sub>0.4</sub>Al<sub>0.3</sub> (RE=La or Mischmetall) by melt spinning.

A melt spinning device with a copper wheel of 30 cm

diameter was used. The influence of the protective gas atmosphere was studied and the cooling rate was changed by a stepwise variation of the gas pressure and the rotational speed (Table 1)

### 2.2. Electrode preparation

The materials were obtained as short ribbons or flakes, immersed in a copper solution as used for electroless deposition and finely ground in a mortar. The resulting powders were supplied with a protective copper layer by chemical reduction. Electrodes were formed by attaching the material to a nickel net using a fluoro-organic binder. A more detailed description of the melt spinning process and the electrode preparation was given in Ref. [1].

Table 1  
Preparation conditions

Basic comp	Gas	Gas pressure /bar	Rotational speed/r.p.m.
I	Ar	1.100/1.000	1500
I	He	1.100/1.000	2000
II	Ar	1.100/1.000	2000
II	He	1.000/0.920	1500
III	Ar	1.100/1.000	2000
III	He	0.990/0.910	2000
I	He	0.650/0.550	2000
II	He	0.660/0.580	2000
III	He	0.640/0.560	2000
I	He	0.350/0.300	1500
I	He	0.160/0.100	1100
II	He	0.160/0.090	2000
III	He	0.160/0.100	2500

Basic compounds: I= $\text{LaNi}_{3.5}\text{Co}_{0.8}\text{Mn}_{0.4}\text{Al}_{0.3}$ ; II= $\text{MmNi}_{3.5}\text{Co}_{0.8}\text{Mn}_{0.4}\text{Al}_{0.3}$ , 30%La in Mm; III= $\text{MmNi}_{3.5}\text{Co}_{0.8}\text{Mn}_{0.4}\text{Al}_{0.3}$ , 50%La in Mm; gas pressure= gas reservoir/meltspinning chamber.

### 2.3. Structure analysis

Structure analysis was carried out by X-ray diffractometry (Siemens D 500) and the Debye–Scherrer method. The average grain size and the influence of lattice distortions were estimated by evaluation of the diffraction line broadening. Additional investigations were done by scanning electron microscopy and transmission electron microscopy.

### 2.4. Storage capacity

The hydrogen storage capacity was determined by mass controlled isothermic absorption of hydrogen at 80 °C.

### 2.5. Electrochemical characterization

Electrochemical measurements were carried out in 6 M KOH using a saturated mercurousulphate reference electrode. The storage capacity was measured by constant current charge/discharge cycles at different current densities.

## 3. Results and discussion

### 3.1. Melt spinning parameters and cooling rate

The efficiency of rapid solidification by melt spinning is determined by different parameters and a nanocrystalline or amorphous state can be achieved only by sufficient cooling rates.

Although the rotational speed and the heat transport inside the copper wheel plays a dominant role, the cooling rate is also influenced by the intensity and time of the contact between the liquid metal and the surface of the copper wheel. The protective gas atmosphere can enhance the contact time and contributes to the cooling process by means of its specific heat and specific thermal conductivity, its viscosity and pressure. The cooling rate was not measured directly but structural changes of samples prepared in helium atmosphere at reduced pressures indicate, that a maximum is obtained at pressures below 300 mbar.

### 3.2. Structural changes by melt spinning

$\text{MmNi}_{3.5}\text{Co}_{0.8}\text{Mn}_{0.4}\text{Al}_{0.3}$  like other  $\text{LaNi}_5$ -related intermetallic compounds crystallize in the hexagonal  $\text{CaCu}_5$ -structure. Previous experiments had shown, that  $\text{LaNi}_5$  and related compounds are difficult to get in an amorphous state. From Debye–Scherrer films a uniform crystalline

phase with a  $\text{CaCu}_5$ -structure could be detected both in samples prepared by induction melting and melt spinning. Apart from a slight line broadening no change of composition or crystal structure was observed in rapidly solidified samples.

SEM pictures of samples produced in helium atmosphere at pressures below 550 mbar showed a needlelike (1–3  $\mu\text{m}$  diameter) texture vertical to the surface of the ribbons or flakes respectively.

A calculation of the grain size by evaluation of the XRD peak broadening yielded values ranging from 25 to 60 nm indicating that the average grain size is lower than the average diameter of the texture profiles by at least one order of magnitude.

Additional examinations using a high resolving TEM revealed that a major part of the material remained in a nanocrystalline state with a grain size significantly below 10 nm. The TEM pictures also showed some isolated grains with a diameter between 10–300 nm embedded in a matrix of nanocrystalline material (Fig. 1).

Samples prepared in Ar atmosphere at a lower cooling rate exhibited a microcrystalline hexagonal structure with a grain size between 0.5 and 3  $\mu\text{m}$ .

A more detailed examination of the XRD patterns additionally revealed significant differences of the intensity distribution. Fig. 2 shows the XRD patterns of  $\text{LaNi}_{3.5}\text{Co}_{0.8}\text{Mn}_{0.4}\text{Al}_{0.3}$  prepared by induction melting (A) and by melt spinning with a lower (B) and a higher (C) cooling rate. Obviously the 002 peak of material (B) is significantly increased. Material (A) shows an intensity distribution similar to the values calculated for  $\text{LaNi}_5$  and (C) shows a less distinct deviation like (B). As the samples (B) and (C) consisted of short ribbons or flakes they were not randomly attached to the carrier like a powder (A). The intensity increase of the 002 peak of (B) is apparently due to a predominant orientation of the *c*-axis of the hexagonal crystals vertical to the surface of the ribbons. A further increase of the cooling rate causes a more random orienta-

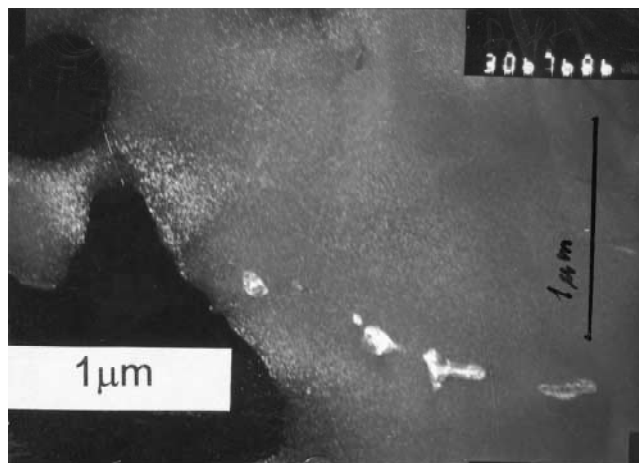


Fig. 1. TEM picture of material (C).

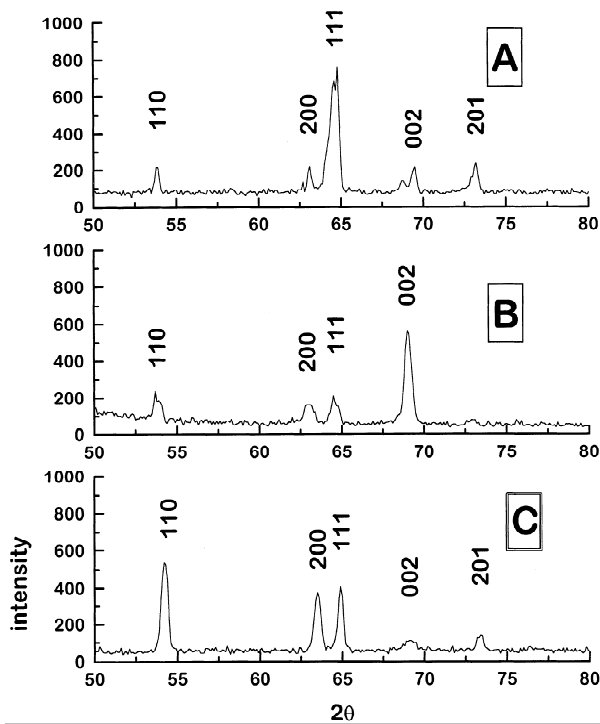


Fig. 2. XRD-patterns of polycrystalline samples before (A) and after meltspinning (B,C) at different cooling rates.

tion of the grains. This finding is in good agreement with the results of high resolution TEM.

Isothermic hydrogen absorption experiments showed only negligible differences in the storage capacities between the materials as supplied and nanocrystalline materials.

### 3.3. Electrochemical behaviour

Nanocrystalline materials (C) generally showed improved discharge characteristics with distinct potential plateaux after a very few activation cycles in comparison to the materials as supplied (A). The improvement of activation behaviour and kinetic properties is probably due

to well established diffusion paths for hydrogen atoms along the numerous grain boundaries. A comparison between the discharge capacities and the corresponding capacity values calculated from isothermic hydrogen desorption experiments showed only negligible differences between the materials as supplied and nanocrystalline materials.

In contrast to that, melt-spun micro-crystalline samples with oriented crystallization (B) showed very poor kinetic properties probably indicating an anisotropy of hydrogen diffusion inside the single crystals.

## 4. Conclusion

Nanocrystalline materials can be prepared from  $AB_5$ -type intermetallic compounds by optimization of the melt spinning process. Electrodes prepared from these materials show excellent activation behaviour and improved electrochemical properties. Microcrystalline material with oriented crystallization prepared at a lower cooling rate exhibits poor kinetic properties.

## Acknowledgments

The investigations were carried out in cooperation with the Institut für Experimentalphysik der Technischen Universität Wien. The TEM pictures were supplied by the Institut für Angewandte und Technische Physik. The author thanks Prof. H. Kirchmayr, Prof. Ch. Fabjan and Doz. P. Pongratz for their encouragement.

## References

- [1] H. Kronberger, *GDCh Monographie, 2, Elektrochemie und Werkstoffe*, GDCh, Frankfurt, 1995, pp. 411–425.
- [2] R. Mishima, H. Miyamura, T. Sakai, N. Kuriyama, H. Ishikawa and I. Uehara, *J. Alloys Comp.*, 192 (1993) 176–178.